

Ground-state cooling based on a three-cavity optomechanical system in the unresolved-sideband regime

Jing Wang(王婧)

Citation: Chin. Phys. B, 2021, 30 (**2**): 024204. DOI: 10.1088/1674-1056/abc159
Journal homepage: http://cpb.iphy.ac.cn; http://iopscience.iop.org/cpb

What follows is a list of articles you may be interested in

Quantum speed limit time and entanglement in a non-Markovian evolution of spin qubits of coupled quantum dots

M. Bagheri Harouni
Chin. Phys. B, 2020, 29 (**12**): 124203. DOI: 10.1088/1674-1056/abab75

Dissipative quantum phase transition in a biased Tavis-Cummings model

Zhen Chen(陈臻), Yueyin Qiu(邱岳寅), Guo-Qiang Zhang(张国强), Jian-Qiang You(游建强)
Chin. Phys. B, 2020, 29 (**4**): 044201. DOI: 10.1088/1674-1056/ab7b55

Double-passage mechanical cooling in a coupled optomechanical system

Qing-Xia Mu(穆青霞), Chao Lang(郎潮), Wen-Zhao Zhang(张闻钊)
Chin. Phys. B, 2019, 28 (**11**): 114206. DOI: 10.1088/1674-1056/ab48f1

Phase-dependent double optomechanically induced transparency in a hybrid optomechanical cavity system with coherently mechanical driving

Shi-Chao Wu(吴士超), Li-Guo Qin(秦立国), Jian Lu(鹿建), Zhong-Yang Wang(王中阳)
Chin. Phys. B, 2019, 28 (**7**): 074204. DOI: 10.1088/1674-1056/28/7/074204

Cavity optomechanics: Manipulating photons and phonons towards the single-photon strong coupling

Yu-long Liu(刘玉龙), Chong Wang(王冲), Jing Zhang(张靖), Yu-xi Liu(刘玉玺)
Chin. Phys. B, 2018, 27 (**2**): 024204. DOI: 10.1088/1674-1056/27/2/024204

Ground-state cooling based on a three-cavity optomechanical system in the unresolved-sideband regime*

Jing Wang(王婧)†

College of Physics, Tonghua Normal University, Tonghua 134000, *China*

(Received 19 August 2020; revised manuscript received 8 September 2020; accepted manuscript online 15 October 2020)

In the unresolved sideband regime, we propose a scheme for cooling mechanical resonator close to its ground state in a three-cavity optomechanical system, where the auxiliary cavities are indirectly connected with the mechanical resonator through standard optomechanical subsystem. The standard optomechanical subsystem is driven by a strong pump laser field. With the help of the auxiliary cavities, the heating process is suppressed and the cooling process of the mechanical resonator is enhanced. More importantly, the average phonon number is much less than 1 in a larger range. This means that the mechanical resonator can be cooled down to its ground state. All these interesting features will significantly promote the physical realization of quantum effects in multi-cavity optomechanical systems.

Keywords: ground-state cooling, three-cavity optomechanical system, unresolved sideband regime

PACS: 42.50.Pq, 42.50.Nn, 42.50.Ct, 03.65.Yz **DOI:** 10.1088/1674-1056/abc159

1. Introduction

As is well known, with the rapid development of microscale integrable devices, cavity optomechanical systems play an important role in quantum information processing.[1–17] A generic optomechanical system consists of a Fabry–Pérot cavity in which one mirror is fixed but the other is free to move around its equilibrium position as a mechanical resonator.[2,3] Using strong pump laser field to drive the cavity field, the effective cavity field length will be changed by the mechanical resonator, resulting in an optical pressure on the mirror which is proportional to the intensity of the trapped cavity field. This mechanism gives the optomechanical coupling between the cavity field and the mechanical resonator.[2,3] In the cavity optomechanical system, researchers can manipulate the cavity field by mechanical resonator to achieve optomechanically induced transparency (OMIT),[2,3] optomechanically induced amplification,[4] coherent perfect absorption or transmission,[5] fast and slow light,[6] optical nonreciprocity,[7,8] etc. The coherent state,[18] superposition state[19] and entangled state[20–22] of mechanical resonator can also be obtained by manipulating a mechanical resonator through cavity field. More recently the sideband scattering engineering has been proposed theoretically and demonstrated theoretically using squeezing, and in particular three different forms of squeezing: (i) injected squeezing,[23] (ii) intracavity squeezing,[24] (iii) in-loop feedback squeezing. However, the realization of these physical phenomena is based on the premise that the mechanical resonator is cooled to the ground state.

Many different cooling schemes have been proposed to realize the ground-state cooling of mechanical resonators.[25–31] One of the famous cooling methods is sideband cooling.[25] This method requires the condition of the resolved sideband regime, where the mechanical resonator resonance frequency is higher than the cavity field decay rate.[25] In practice, it is a challenging task to satisfy this condition for a typical mechanical resonator whose frequency is in the range of kHz–MHz. Therefore, it is particularly important to realize ground-state cooling of mechanical resonator in the unresolved sideband regime, in which the cavity field decay rate would be larger than the resonance frequency of the mechanical resonator. In recent years, researchers have made some achievements in the unresolved sideband regime. For example, the electromagnetically induced transparency (EIT)-like cooling mechanism. It is based on quantum interference cooling mechanical resonator to its the ground state.[26] Guo and Li[26] propose to cool a mechanical resonator close to its ground state via an EIT-like cooling mechanism. With the help of the auxiliary cavity field whose decay rate is less than the frequency of the mechanical resonator, the cooling process of the double-cavity optomechanical system corresponds to the maximum value of the optical fluctuation spectrum and the heating process corresponds to the minimum value of the optical fluctuation spectrum by selecting the optimal parameters. Results show that the cooling effect of the double-cavity optomechanical system is better than that of the standard cavity optomechanical system, even it can be cooled to the ground-state cooling. Inspired by Ref. [26] we naturally ask a question: Can ground-state cooling of a mechanical resonator be achieved in a multi-cavity optomechanical system? Can the multi-cavity optical mechanical system bring new insights into the ground-state cooling of a mechanical resonator?

In this paper, under the unresolved sideband condition,

*Project supported by the Research Fund of Tonghua Normal University (Grant No. 202017ND).

†Corresponding author. E-mail: pwl1207wj@163.com

© 2021 Chinese Physical Society and IOP Publishing Ltd

we address the above questions by investigating the ground-state cooling of a mechanical resonator via an EIT-like cooling mechanism in a three-cavity optomechanical system. The three-cavity optomechanical system under consideration is schematically shown in Fig. 1. The system includes 3 cavity fields labeled by c_1, c_2, and c_3. We let only c_1 interact with the mechanical resonator by radiation pressure. Thus c_1 forms a standard optomechanical subsystem. Two adjacent cavities are coupled to each other. In addition, c_1 is driven by a pump laser field. In the system we consider, there are two different quantum interference effect channels. One is from c_1–c_2 coupling and the other is from c_1–c_3 coupling. Two different quantum interference effect channels satisfy the condition of two-photon resonance, respectively. By modifying the quantum interference, the cooling process can be enhanced while the heating process can be suppressed, so that the ground-state cooling of mechanical resonator can be realized. It should be noted that the results obtained are similar to Refs. [26–28]. However, this study is different from Ref. [26–28]. First, the physical model is different. The physical model of Ref. [26] is a double-cavity optomechanical system, the physical model of Ref. [27] is a double-Lagureer–Gaussian-cavity optomechanical system, while the physical model of Ref. [28] is a double-cavity optomechanical system containing an atomic ensemble. Our scheme is to realize the ground-state cooling of the mechanical resonator in the multi-cavity optomechanical system. Second, in Ref. [26], the auxiliary cavity field must be a good cavity field, while in our scheme, the auxiliary cavity fields can be bad cavity fields. Third, the additional auxiliary cavity fields not only change the quantum interference effect channels, but also have more adjustable parameters, which can better adjust the cooling effect. Here instead of only illustrating the ground-state cooling of mechanical resonator in such a system, we are especially interested in what roles the c_1, c_2, c_3 could play. It is also helpful for realizing the physics of the three-cavity optomechanical system. Fourth, our scheme can make the mean phonon number close to zero in a larger range of parameters.

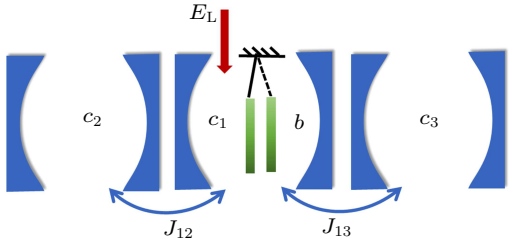


Fig. 1. The schematic of a three-cavity optomechanical system. Three cavities connected through tunneling parameters J_{12} (J_{13}). A strong pump light field is injected into cavity c_1 while cavity c_1 is coupled with mechanical resonator b.

The paper is organized as follows. Firstly, we introduce the theoretical model, the detailed analytical expressions of the system, obtain the steady-state mean values, and discuss the final mean phonon number. Secondly, we study in detail the ground-state cooling of mechanical resonators by tuning the system parameters and provide the corresponding physics explanation. Lastly, we summarize our work.

2. Model and equations

We consider a hybrid system, composed of three cavities c_j ($j = 1,2,3$), a mechanical resonator b, as shown in Fig. 1. The c_1 is coupled to the mechanical resonator via the radiation pressure force. Furthermore, c_1 is directly coupled to c_2 (c_3). The c_1 is simultaneously driven by a single-frequency continuous-wave classical input field, which is called the pump laser field. Firstly, by setting $\hbar = 1$, the total Hamiltonian of this hybrid system in the presence of a pump laser field can be written as an added mechanical resonator free term and optomechanical interaction on the basis of ordinary cavity Hamiltonian, i.e.,[32–36]

$$H = \sum_{j=1}^{3} \omega_j c_j^\dagger c_j + \omega_{\rm m} b^\dagger b - g_0(b^\dagger + b)c_1^\dagger c_1 + J_{12}(c_1^\dagger c_2 + c_2^\dagger c_1) + J_{13}(c_1^\dagger c_3 + c_1^\dagger c_3) + {\rm i}(E_{\rm L} c_1^\dagger {\rm e}^{-{\rm i}\omega_{\rm L} t} - E_{\rm L}^* c_1 {\rm e}^{{\rm i}\omega_{\rm L} t}). \quad (1)$$

In Eq. (1), the first term denotes the energy of the three cavity fields with the creation (annihilation) operator $c_j^\dagger$ (c_j), resonance frequency ω_j, and decay rate κ_j ($j = 1,2,3$). The second term represents the free Hamiltonian of the mechanical resonator with creation (annihilation) operator $b^\dagger$ (b), resonance frequency $\omega_{\rm m}$, effective mass m. The third term shows the interaction between the c_1 and b with optomechanical coupling strength $g_0 = \frac{\omega_1}{L}\sqrt{1/2m\omega_{\rm m}}$, and L is length of the c_1. The next two terms give the interaction between the c_1 and c_2 (c_3), with J_{12} (J_{13}) being the coupling strength. The J_{12}, as well as J_{13}, can be efficiently modulated by the distance between c_1 and c_2. Finally, the last term describes the the optical driving with frequencies $\omega_{\rm L}$. The parameter $E_{\rm L} = \sqrt{2Pk_1/\omega_{\rm L}}$ is the amplitude of the pump laser field, which is related to the pump laser power P. Without loss of generality, we have assumed g_0, J_{12} (J_{13}) and $E_{\rm L}$ to be real numbers.

Transforming the Hamiltonian Eq. (1) into the rotating frame at the frequency $\omega_{\rm L}$ of the pump laser field by means of $H_1 = \sum_{j=1}^{3} \omega_{\rm L} c_j^\dagger c_j$, $U_t = {\rm e}^{-{\rm i}H_1 t}$ and $H_{\rm rotating} = U_t^\dagger H U_t - {\rm i}U_t^\dagger \frac{\partial U_t}{\partial t} = U_t^\dagger (H - H_1) U_t$, the resulting Hamiltonian Eq. (1) can be derived as

$$\begin{aligned} H_{\rm rotating} &= \Delta_{11} c_1^\dagger c_1 + \Delta_2 c_2^\dagger c_2 + \Delta_3 c_3^\dagger c_3 \\ &\quad + \omega_{\rm m} b^\dagger b - g_0(b^\dagger + b)c_1^\dagger c_1 \\ &\quad + J_{12}(c_1^\dagger c_2 + c_2^\dagger c_1) + J_{13}(c_1^\dagger c_3 + c_1^\dagger c_3) \\ &\quad + {\rm i}(E_{\rm L} c_1^\dagger - E_{\rm L}^* c_1), \end{aligned} \quad (2)$$

where $\Delta_{11} = \omega_1 - \omega_{\rm L}$, $\Delta_2 = \omega_2 - \omega_{\rm L}$, and $\Delta_3 = \omega_3 - \omega_{\rm L}$ are the detuning of the j-th ($j = 1,2,3$) cavity field frequency with pump laser field frequency. Note that the same cavity resonance frequencies $\omega_1 = \omega_2 = \omega_3$ lead to the same detuning $\Delta_{11} = \Delta_2 = \Delta_3$.

According to the Heisenberg equation and the commutation relation, the temporal evolution of the operators c_1, c_2, c_3 and b can be obtained. Taking the decay terms into consideration, we can obtain the Heisenberg equations as follows:

$$\begin{aligned}
\partial_t c_1 &= -(\kappa_1+\mathrm{i}\Delta_{11})c_1-\mathrm{i}J_{12}c_2-\mathrm{i}J_{13}c_3\\
&\quad +E_{\mathrm{L}}+\mathrm{i}g_0(b^\dagger+b)c_1+\sqrt{2\kappa_1}c_1^{\mathrm{in}}(t),\\
\partial_t c_2 &= -(\kappa_2+\mathrm{i}\Delta_2)c_2-\mathrm{i}J_{12}c_1+\sqrt{2\kappa_2}c_2^{\mathrm{in}}(t),\\
\partial_t c_3 &= -(\kappa_3+\mathrm{i}\Delta_3)c_3-\mathrm{i}J_{13}c_1+\sqrt{2\kappa_3}c_3^{\mathrm{in}}(t),\\
\partial_t b &= -(\gamma_{\mathrm{m}}+\mathrm{i}\omega_{\mathrm{m}})b+\mathrm{i}g_0c_1^\dagger c_1+\sqrt{2\gamma_{\mathrm{m}}}b^{\mathrm{in}}(t). \qquad (3)
\end{aligned}$$

Here γ_{m} is the decay rate of mechanical resonator; $c_j^{\mathrm{in}}(t)$ and $b^{\mathrm{in}}(t)$ are the input quantum vacuum noise operator in the j-th $(j=1,2,3)$ cavity field and thermal noise on the mechanical resonator.[37]

Defining the steady solution of the cavity field and mechanical resonator as C_j $(j=1,2,3)$ and B, respectively, by solving Eq. (3), we can obtain the steady solutions as follows:

$$\begin{aligned}
C_1 &= \frac{E_{\mathrm{L}}}{\kappa_1+\mathrm{i}\Delta_1+\frac{J_{12}^2}{\kappa_2+\mathrm{i}\Delta_2}+\frac{J_{13}^2}{\kappa_3+\mathrm{i}\Delta_3}},\\
C_2 &= -\frac{\mathrm{i}J_{12}C_1}{\kappa_2+\mathrm{i}\Delta_2},\\
C_3 &= -\frac{\mathrm{i}J_{13}C_1}{\kappa_3+\mathrm{i}\Delta_3},\\
B &= \frac{\mathrm{i}g_0|C_1|^2}{\gamma_{\mathrm{m}}+\mathrm{i}\omega_{\mathrm{m}}}, \qquad (4)
\end{aligned}$$

where $\Delta_1=\Delta_{11}-g_0(B^*+B)$ is the effective detuning between the c_1 and the the pump field, including the frequency shift caused by the mechanical resonator motion.

Generally, in the case of strong pump laser field, linearizing the operators around the steady state values as $c_j=C_j+\delta c_j$ $(j=1,2,3)$, $b=B+\delta b$. Neglecting the constant and higher-order terms with $|C_1|\gg 1$, Eq. (3) then becomes

$$\begin{aligned}
\partial_t\delta c_1 &= -(\kappa_1+\mathrm{i}\Delta_1)\delta c_1-\mathrm{i}J_{12}\delta c_2\\
&\quad -\mathrm{i}J_{13}\delta c_3+\mathrm{i}g(\delta b^\dagger+\delta b)+\sqrt{2\kappa_1}c_1^{\mathrm{in}},\\
\partial_t\delta c_2 &= -(\kappa_2+\mathrm{i}\Delta_2)\delta c_2-\mathrm{i}J_{12}\delta c_1+\sqrt{2\kappa_2}c_2^{\mathrm{in}},\\
\partial_t\delta c_3 &= -(\kappa_3+\mathrm{i}\Delta_3)\delta c_3-\mathrm{i}J_{13}\delta c_1+\sqrt{2\kappa_3}c_3^{\mathrm{in}},\\
\partial_t\delta b &= -(\gamma_{\mathrm{m}}+\mathrm{i}\omega_{\mathrm{m}})\delta b+\mathrm{i}g\left(\delta c_1+\delta c_1^\dagger\right)+\sqrt{2\gamma_{\mathrm{m}}}b^{\mathrm{in}}. \qquad (5)
\end{aligned}$$

The $g=g_0C_1$ is the enhanced effective optomechanical coupling coefficient.

We can make an inversion based on Eq. (5) and obtain the following Hamiltonian:

$$\begin{aligned}
H &= \Delta_1\delta c_1^\dagger\delta c_1+\Delta_2\delta c_2^\dagger\delta c_2+\Delta_3\delta c_3^\dagger\delta c_3\\
&\quad +\omega_{\mathrm{m}}\delta b^\dagger\delta b-g(\delta b^\dagger+\delta b)\left(\delta c_1^\dagger+\delta c_1\right)\\
&\quad +J_{12}(\delta c_1^\dagger\delta c_2+\delta c_2^\dagger\delta c_1)+J_{13}(\delta c_1^\dagger\delta c_3+\delta c_3^\dagger\delta c_1). \qquad (6)
\end{aligned}$$

In the regime $g\ll\omega_{\mathrm{m}}$, we can ignore the back actions of the mechanical resonator. Therefore, in Eq. (6), the effective Hamiltonian for cooling reads

$$\begin{aligned}
H_{\mathrm{cooling}} &= \Delta_1\delta c_1^\dagger\delta c_1+\Delta_2\delta c_2^\dagger\delta c_2+\Delta_3\delta c_3^\dagger\delta c_3\\
&\quad +J_{12}(\delta c_1^\dagger\delta c_2+\delta c_2^\dagger\delta c_1)\\
&\quad +J_{13}(\delta c_1^\dagger\delta c_3+\delta c_3^\dagger\delta c_1). \qquad (7)
\end{aligned}$$

The Heisenberg equations of Hamiltonian (7) are presented as follows:

$$\begin{aligned}
\partial_t\delta c_1 &= -(\kappa_1+\mathrm{i}\Delta_1)\delta c_1-\mathrm{i}J_{12}\delta c_2-\mathrm{i}J_{13}\delta c_3+\sqrt{2\kappa_1}c_1^{\mathrm{in}},\\
\partial_t\delta c_2 &= (\kappa_2+\mathrm{i}\Delta_2)\delta c_2-\mathrm{i}J_{12}\delta c_1+\sqrt{2\kappa_2}c_2^{\mathrm{in}},\\
\partial_t\delta c_3 &= (\kappa_3+\mathrm{i}\Delta_3)\delta c_3-\mathrm{i}J_{13}\delta c_1+\sqrt{2\kappa_3}c_3^{\mathrm{in}}. \qquad (8)
\end{aligned}$$

We define the radiation force as[26–28]

$$F=\delta c_1^\dagger+\delta c_1. \qquad (9)$$

The optical force fluctuation spectrum for this force is[26–28]

$$S_{\mathrm{FF}}(\omega)=\int \mathrm{d}t\,\mathrm{e}^{\mathrm{i}\omega t}\langle F(t)F(0)\rangle. \qquad (10)$$

By introducing the Fourier transform of the operators

$$\begin{aligned}
f(\omega) &= \frac{1}{\sqrt{2\pi}}\int_{-\infty}^{+\infty}\mathrm{e}^{\mathrm{i}\omega t}f(t)\,\mathrm{d}t,\\
f(t) &= \frac{1}{\sqrt{2\pi}}\int_{-\infty}^{+\infty}\mathrm{e}^{-\mathrm{i}\omega t}f(\omega)\,d\omega, \qquad (11)
\end{aligned}$$

we can obtain the following two important properties of Fourier transform:

$$\begin{aligned}
f^\dagger(-\omega) &= \frac{1}{\sqrt{2\pi}}\int_{-\infty}^{+\infty}\mathrm{e}^{\mathrm{i}\omega t}f^\dagger(t)\,\mathrm{d}t,\\
-\mathrm{i}\omega f(\omega) &= \frac{1}{\sqrt{2\pi}}\int_{-\infty}^{+\infty}\mathrm{e}^{\mathrm{i}\omega t}\dot{f}(t)\,\mathrm{d}t. \qquad (12)
\end{aligned}$$

The c_j^{in} and $c_j^{\mathrm{in}\dagger}$ associated with the j-th $(j=1,2,3)$ cavity obey the relation

$$\left\langle c_j^{\mathrm{in}}(\omega)c_j^{\mathrm{in}\dagger}(-\omega')\right\rangle=\delta(\omega+\omega'),\ \ (j=1,2,3). \qquad (13)$$

We can reach

$$S_{\mathrm{FF}}(\omega)=\frac{2\kappa_1+2\kappa_2|B(\omega)|^2+2\kappa_3|D(\omega)|^2}{|A(\omega)|^2}, \qquad (14)$$

where

$$\begin{aligned}
A(\omega)&=\kappa_1+\mathrm{i}(\Delta_1-\omega)+\frac{J_{12}^2}{\kappa_2+\mathrm{i}(\Delta_2-\omega)}+\frac{J_{13}^2}{\kappa_3+\mathrm{i}(\Delta_3-\omega)},\\
B(\omega)&=-\frac{\mathrm{i}J_{12}}{\kappa_2+\mathrm{i}(\Delta_2-\omega)},\quad D(\omega)=-\frac{\mathrm{i}J_{13}}{\kappa_3+\mathrm{i}(\Delta_3-\omega)}.
\end{aligned}$$

If we further simplify $S_{\mathrm{FF}}(\omega)$, we can obtain

$$S_{\mathrm{FF}}(\omega)=\frac{1}{A(\omega)}+\frac{1}{A^*(\omega)}. \qquad (15)$$

The rate equation for the phonon on the mechanical resonator is given by [26–28,38]

$$\dot{P}_n=\Gamma_{n\leftarrow n+1}P_{n+1}+\Gamma_{n\leftarrow n-1}P_{n-1}-\Gamma_{n-1\leftarrow n}P_n$$

$$-\Gamma_{n+1\leftarrow n}P_n+\gamma_{\rm m}(n_{\rm m}+1)(n+1)P_{n+1}$$
$$+\gamma_{\rm m}n_{\rm m}nP_{n-1}-\gamma_{\rm m}(n_{\rm m}+1)nP_n$$
$$-\gamma_{\rm m}n_{\rm m}(n+1)P_n, \tag{16}$$

where P_n is the probability for the mechanical resonator in the Fock state $|n\rangle$. The first four terms in Eq. (16) caused by the effective optomechanical coupling, the $\Gamma_{n'\leftarrow n}$ refers to the transition rate from the Fock state $|n\rangle$ to $|n'\rangle$, and by using Fermi's golden rule,[26–28,38] we can achieve the transition rate $\Gamma_{n\leftarrow n+1}=(n+1)g^2S_{\rm FF}(\omega_{\rm m})$ (anti-Stokes scattering process) and $\Gamma_{n+1\leftarrow n}=(n+1)g^2S_{\rm FF}(-\omega_{\rm m})$ (Stokes scattering process). The last four terms in Eq. (16) describe the transition induced by the thermal bath. Here $n_{\rm m}$ is the thermal phonon number. Equation (16) can also be rewritten as

$$\dot{P}_n = \gamma_{\rm f}(n_{\rm f}+1)(n+1)P_{n+1}+\gamma_{\rm f}n_fnP_{n-1}-\gamma_{\rm f}(n_{\rm f}+1)nP_n$$
$$-\gamma_{\rm f}n_{\rm f}(n+1)P_n, \tag{17}$$

where $\gamma_{\rm f}$ is the rate at which the average phonon number tends to the steady value $B^{\dagger}B$, which satisfies

$$\gamma_{\rm f}(n_{\rm f}+1)=\gamma_{\rm m}(n_{\rm m}+1)+g^2S_{\rm FF}(\omega_{\rm m}),$$
$$\gamma_{\rm f}n_{\rm f}=\gamma_{\rm m}n_{\rm m}+g^2S_{\rm FF}(-\omega_{\rm m}), \tag{18}$$

$n_{\rm f}$ is the final mean phonon number of the mechanical resonator. If $n_{\rm f}<1$, it should be considered that the mechanical resonator is cooled to the ground state. Solving Eq. (18), the $n_{\rm f}$ can be obtained as

$$n_{\rm f}=\frac{\gamma_{\rm m}n_{\rm m}+\gamma_{\rm c}n_{\rm c}}{\gamma_{\rm m}+\gamma_{\rm c}}, \tag{19}$$

where

$$\gamma_{\rm c}=g^2\left[S_{\rm FF}(+\omega_{\rm m})-S_{\rm FF}(-\omega_{\rm m})\right], \tag{20}$$
$$n_{\rm c}=\frac{S_{\rm FF}(-\omega_{\rm m})}{S_{\rm FF}(\omega_{\rm m})-S_{\rm FF}(-\omega_{\rm m})}. \tag{21}$$

The $n_{\rm f}$ is mainly determined by the $\gamma_{\rm m}$, $n_{\rm m}$, $\gamma_{\rm c}$ and $n_{\rm c}$; $\gamma_{\rm c}$ is the cooling rate and $n_{\rm c}$ is the quantum limit of cooling. If $\gamma_{\rm m}\to 0$, then $n_{\rm f}\to n_{\rm c}$. This means that the $n_{\rm f}$ will have a non-zero lower limit $n_{\rm c}$ even if there is no heat reservoir. In order to obtain very small $n_{\rm f}$, a large cooling rate $\gamma_{\rm c}$ and a small cooling limit $n_{\rm c}$ must be satisfied. The $\gamma_{\rm c}$ and $n_{\rm c}$ are determined by the positive-frequency and negative-frequency parts of the optical fluctuation spectrum, i.e., $S_{\rm FF}(\pm\omega_{\rm m})$. We also note that the negative frequency part of the $S_{\rm FF}(-\omega_{\rm m})$ associated with transition rate $\Gamma_{n+1\leftarrow n}$ determines the heating process, while the positive frequency part of the $S_{\rm FF}(\omega_{\rm m})$ associated with transition rate $\Gamma_{n\leftarrow n+1}$ determines the cooling process. Therefore, in order to make the mechanical resonator cooling close to its ground state, it is necessary to suppress the heating process and to strengthen the cooling process.

3. Ground-state cooling of mechanical resonator

We hope that the ground-state cooling of the mechanical resonator can be achieved in the unresolved sideband regime by introducing the auxiliary cavities (the second and third cavity field), although the auxiliary cavities and the mechanical resonator are indirectly related. Thus in this section, we describe in detail how the auxiliary cavities impact the optical fluctuation spectrum.

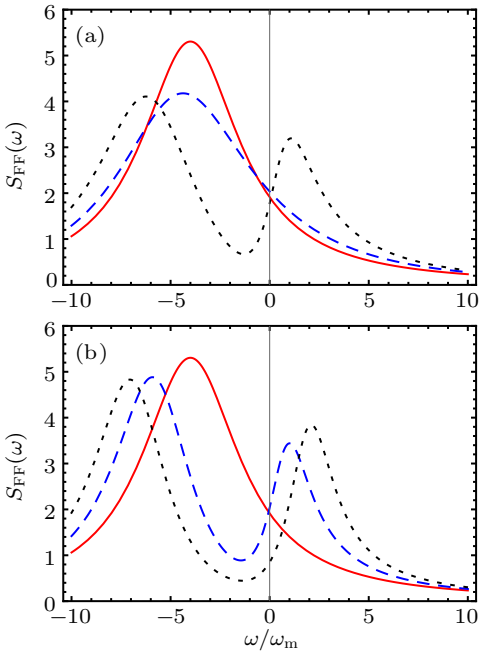


Fig. 2. The optical fluctuation spectrum $S_{\rm FF}(\omega)$ (in arbitrary units) versus the frequency ω: (a) $\kappa_2=10\omega_{\rm m}$, (b) $\kappa_2=0.7\omega_{\rm m}$. Three cases are shown with different colors: (i) the red solid curve shows the $J_{12}=J_{13}=0$, (ii) the blue dashed curve shows the $J_{12}=3\omega_{\rm m}$, $J_{13}=0$, (iii) the black dotted curve shows the $J_{12}=3\omega_{\rm m}$, $J_{13}=3\omega_{\rm m}$. The values of the other parameters are set as $\Delta_1=-4\omega_{\rm m}$, $\Delta_2=\Delta_3=-\omega_{\rm m}$, $\kappa_1=3\omega_{\rm m}$, $\kappa_3=0.5\omega_{\rm m}$.

We first analyze and discuss the influence of decay rate of cavity field c_2 on the ground-state cooling of mechanical resonator. In Fig. 2, from top to bottom, we draw the optical fluctuation spectrum $S_{\rm FF}(\omega)$ versus the frequency ω when c_2 is bad cavity field and c_2 is good cavity field. It is well known that the decay rate determines the quality factor of the cavity field. For c_2 in the bad cavity field case, we adopt the decay rate $\kappa_2=10\omega_{\rm m}$ in Fig. 2(a). For c_2 in the good cavity field case plotted in Fig. 2(b), we have adjusted c_2 to the decay rate of $\kappa_2=0.7\omega_{\rm m}$. For comparison, three cases are plotted for each the optical fluctuation spectrum $S_{\rm FF}(\omega)$: (i) the red solid curve show the $J_{12}=J_{13}=0$, (ii) the blue dashed curve show the $J_{12}=3\omega_{\rm m}$, $J_{13}=0$, (iii) black dotted curve show the $J_{12}=3\omega_{\rm m}$, $J_{13}=3\omega_{\rm m}$. It should be emphasized that under any circumstances, c_1 works in the unresolved sideband regime, i.e., the decay rate of c_1 is much larger than the frequency of b ($\kappa_1>\omega_{\rm m}$). Let us first see the red solid line of Figs. 2(a) and 2(b). When c_2 (c_3) is decoupled from c_1 ($J_{12}=J_{13}=0$), no matter whether c_2 is good or bad, the profile of the $S_{\rm FF}(\omega)$ has a Lorentzian shape with

a single peak located at $\omega = \Delta_1 = -4\omega_m$ and the half width of the peak being κ_1. The values of $S_{FF}(-\omega_m)$ and $S_{FF}(\omega_m)$ are very close. According to the second part of the paper, we know that the optical fluctuation spectrum $S_{FF}(-\omega_m)$ represents the heating process and the optical fluctuation spectrum $S_{FF}(\omega_m)$ represents the cooling process, and $n_f > 1$, so it is impossible to cool the mechanical resonator in the ground state only when c_1 exists. Next, let us see the blue dashed curve ($J_{12} = 3\omega_m$, $J_{13} = 0$). When c_3 and c_1 are decoupled, if c_2 is a bad cavity, the optical fluctuation spectrum $S_{FF}(\omega)$ will still be a Lorentzian shape [see Fig. 2(a)]. On the contrary, when c_2 is a good cavity, we must point out that the system at this time is consistent with Ref. [26], the optical fluctuation spectrum $S_{FF}(\omega)$ becomes distorted, the single Lorentzian peak splits into two asymmetric narrow peaks and a dip emerges between them [see Fig. 2(b)]. The peak on the right hand is in the positive-frequency part of the optical fluctuation spectrum, and the dip is in the negative-frequency part of the optical fluctuation spectrum. The values of $S_{FF}(-\omega_m)$ and $S_{FF}(\omega_m)$ are very different, and $n_f < 1$, that is to say, the asymmetric heating and cooling rates make it possible to realize ground-state cooling of mechanical resonator. It is noteworthy that the dip is caused by EIT.[26–28] Finally, let us see the black dotted curve. When c_2 and c_3 are present ($J_{12} = 3\omega_m$, $J_{13} = 3\omega_m$), no matter whether c_2 is bad (Fig. 2(a) $\kappa_2 = 10\omega_m$) or good (Fig. 2(b) $\kappa_2 = 0.7\omega_m$), the ground-state cooling of the mechanical resonator can be achieved. By comparing Figs. 2(a) and 2(b), the following results can be obtained: due to the introduction of the two auxiliary cavities (both cavities are good or only one of them is good), the mechanical resonator can be successfully cooled to the ground state beyond the resolved sideband condition. At the same time, we also find that participation of the third cavity field can make the cooling mechanism become more efficient in the unresolved sideband regime. Therefore, we can use the method of increasing the number of cavity field to enhance the cooling effect, while to overcome the heating effect.

In the following, we focus on optimal cooling regime when $\kappa_2 > \omega_m$. From Heisenberg Eq. (8), we have

$$\begin{aligned} E_1 &= \frac{1}{2}(\Delta_3 + \Delta_1 + \sqrt{4(J_{12}^2 + J_{13}^2) + (\Delta_3 - \Delta_1)^2}), \\ E_2 &= \frac{1}{2}(\Delta_3 + \Delta_1 - \sqrt{4(J_{12}^2 + J_{13}^2) + (\Delta_3 - \Delta_1)^2}), \\ E_3 &= \Delta_3. \end{aligned} \tag{22}$$

This implies that the three eigen-energies correspond to three inflection points in the optical fluctuation spectrum $S_{FF}(\omega)$. When $\Delta_3 = -\omega_m$, the minimum value in the optical fluctuation spectrum $S_{FF}(\omega)$ can be guaranteed to appear at the position of $\omega = -\omega_m$, so that the heating process can be effectively suppressed. In order to strengthen the cooling process, it is necessary to ensure $E_2 = \omega_m$. Then, we can reach the optimal condition $J_{12}^2 + J_{13}^2 = 2\omega_m(\omega_m - \Delta_1)$.[26–28]

In Fig. 3 we plot the optical fluctuation spectrum $S_{FF}(\omega)$ as a function of the frequency ω for different tunnel decay rate κ_3: $\kappa_3 = 2\omega_m$ (red solid curve), $\kappa_3 = \omega_m$ (blue dashed curve), $\kappa_3 = 0.5\omega_m$ (green dot-dashed curve), $\kappa_3 = 0.05\omega_m$ (black dotted curve). Here we choose $J_{13} = 3\omega_m$ and $\Delta_1 = -4\omega_m$, which means that the optimal coupling strength between the c_1 and c_2 is $J_{12} = \omega_m$. Under the optimal condition, from Fig. 3, we can see that the dip of the optical fluctuation spectrum $S_{FF}(\omega)$ is at $\omega = -\omega_m$ and the peak on the right hand is at $\omega = \omega_m$ even if $\kappa_3 = 2\omega_m$. With the decrease of decay rate κ_3, $S_{FF}(\omega_m)$ is further enlarged, and $S_{FF}(-\omega_m)$ is further suppressed. This is due to the fact that the quantum interference of c_1-c_3 coupling inhibits the heating process. According to Eq. (21), the larger the $S_{FF}(\omega_m)$, the smaller the $S_{FF}(-\omega_m)$, and the better the effect of the ground-state cooling. With decreasing values of decay rate κ_3 to $0.05\omega_m$, the optical fluctuation spectrum value for the heating process can reach zero completely ($S_{FF}(-\omega_m) \simeq 0$), the cooling process can reach its maximal value ($S_{FF}(\omega_m) = 5$). This means that in the three-cavity system, the smaller decay rate κ_3 is more suitable for ground-state cooling the mechanical resonator.

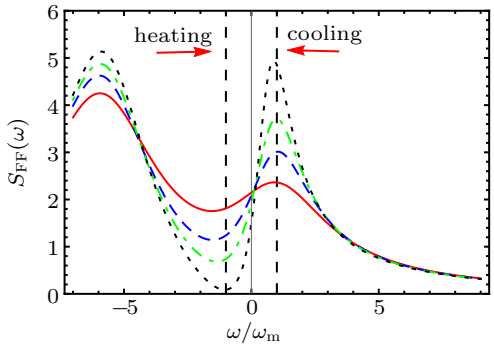


Fig. 3. The optical fluctuation spectrum $S_{FF}(\omega)$ (in arbitrary units) versus ω, for $\kappa_3 = 2\omega_m$ (red solid curve), $\kappa_3 = \omega_m$ (blue dashed curve), $\kappa_3 = 0.5\omega_m$ (green dot-dashed curve), $\kappa_3 = 0.05\omega_m$ (black dotted curve). Here, $\kappa_2 = 10\omega_m$, $J_{13} = 3\omega_m$, $J_{12} = \sqrt{2\omega_m(\omega_m - \Delta_1) - J_{13}^2}$. For the other parameters see Fig. 2.

Figures 2 and 3 highlight the key role of the decay rate $\kappa_{2,3}$ in observing the ground-state cooling phenomena. In order to accurately explain the effect of decay rate κ_3 on the ground-state cooling of the mechanical resonator, we plot the optical fluctuation spectrum $S_{FF}(\omega)$ as a function of decay rate κ_3 at $\omega = -\omega_m$ (red curve) and $\omega = \omega_m$ (blue dashed curve) in Fig. 4. It is found that the heating effect monotonously increases with the decay rate κ_3, the cooling effect is just the opposite. In the regime $0 < \kappa_3 < 3\omega_m$, we have $S_{FF}(-\omega_m) < S_{FF}(\omega_m)$, whereas $S_{FF}(\omega_m) < S_{FF}(-\omega_m)$ when $3\omega_m < \kappa_3 < 4\omega_m$. Therefore, in order for the ground state of the mechanical oscillator to be good, the decay rate κ_3 must be small enough. This is consistent with Fig. 3.

Figure 5 shows the variations of the cooling rate γ_c as a function of J_{13}. The red curve $\kappa_3 = 0.01\omega_m$, blue dashed curve $\kappa_3 = 0.5\omega_m$, green dot-dashed curve $\kappa_3 = 2\omega_m$. As you can

see from Fig. 5, if you want to cooling rate faster, the value of κ_3 will be smaller.

Figure 6 shows the variation of the steady-state final mean phonon number $n_{\rm f}$ of the mechanical resonator as a function of J_{13}. One can clearly see that the $n_{\rm f}$ can be less than 1. This means that mechanical resonator can be cooled nearly to its ground state, even in the usual unresolved sidebands, due to the presence of the auxiliary cavities.

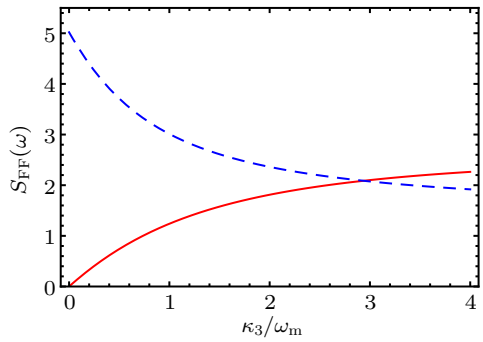


Fig. 4. The optical fluctuation spectrum $S_{\rm FF}(\omega)$ (in arbitrary units) versus κ_3 with $\omega = -\omega_{\rm m}$ (red solid curve) and $\omega = \omega_{\rm m}$ (blue dashed curve). For the other parameters see Fig. 2.

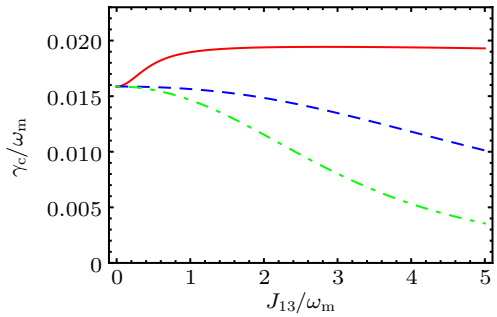


Fig. 5. The cooling rate $\gamma_{\rm c}$ as a function of J_{13} in the case of $\Delta_1 = \omega_{\rm m} - \frac{J_{12}^2+J_{13}^2}{2\omega_{\rm m}}$ for three different κ_3 with $\kappa_3 = 2\omega_{\rm m}$ (green dotdashed curve), $\kappa_3 = 0.5\omega_{\rm m}$ (blue dashed curve), $\kappa_3 = 0.01\omega_{\rm m}$ (red solid curve). Here $\omega_{\rm m} = 4\pi \times 10 \times 10^6$ Hz, $g = 0.2\omega_{\rm m}$. For the other parameters see Fig. 2.

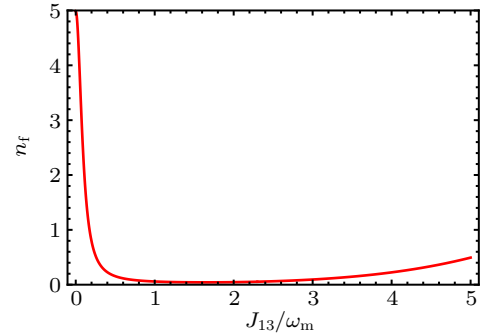


Fig. 6. The mean phonon number $n_{\rm f}$ as a function of the J_{13} in the case of $\Delta_1 = \omega_{\rm m} - \frac{J_{12}^2+J_{13}^2}{2\omega_{\rm m}}$ for $J_{12} = \gamma_{\rm m}$. Here $\gamma_{\rm m} = 5\pi \times 10^2$ Hz, $g_0 = 1.6 \times 10^{-4}\omega_{\rm m}$, $E_{\rm L} = 6000\omega_{\rm m}$. For the other parameters see Fig. 2.

4. Conclusions

We have studied the ground-state cooling of the mechanical resonators in a coupled cavity optomechanical system. The optical fluctuation spectrum can be modified by quantum interference effects induced by the c_1–c_2 and c_1–c_3 couplings. Because of the combination of two quantum interference effects, by selecting the optimal parameters, the cooling process of the mechanical resonator corresponds to the maximum value of the optical fluctuation spectrum, and the heating process corresponds to the minimum value of the optical fluctuation spectrum, which finally cools the mechanical resonator.

References

[1] Yan X B 2020 *Phys. Rev. A* **101** 043820
[2] Weis S, Rivière R, Deleglise S, Gavartin E, Arcizet O, Schliesser A and Kippenberg T J 2011 *Science* **330** 1520
[3] Agarwal G S and Huang S M 2010 *Phys. Rev. A* **81** 041803
[4] Yang Q, Hou B P and Lai D G 2017 *Opt. Express* **25** 9697
[5] Yan X B 2005 *arXiv:2005.11871 [quant-ph]*
[6] Gu K H, Yan X B, Zhang Y, Fu C B, Liu Y M, Wang X and Wu J H 2015 *Opt. Commun.* **338** 569
[7] Xia C C, Yan X B, Tian X D and Gao F 2019 *Opt. Commun.* **451** 197
[8] Wang J 2020 *Chin. Phys. B* **29** 034210
[9] Lu T X, Jiao Y F, Zhang H L, Saif F and Jing H 2019 *Phys. Rev. A* **100** 013813
[10] Jiao Y F, Lu T X and Jing H 2018 *Phys. Rev. A* **97** 013843
[11] Wu Q 2016 *Chin. Phys. B* **25** 010304
[12] Jiang C, Song L N and Li Y 2019 *Phys. Rev. A* **99** 023823
[13] Xu X W, Song L N, Zheng Q, Wang Z H and Li Y 2018 *Phys. Rev. A* **98** 063845
[14] Chen H J 2019 *EPJ Quantum Technol.* **6** 3
[15] He B, Yang L and Jiang X S 2018 *Phys. Rev. Lett.* **120** 203904
[16] Yan X B 2017 *Phys. Rev. A* **96** 053831
[17] Yan X B, Lu H L, Gao F and Yang L 2019 *Front. Phys.* **14** 52601
[18] Rabl P, Genes C, Hammerer K, Aspelmeyer M 2009 *Phys. Rev. A* **80** 063819
[19] Marshall W, Simon C, Penrose R and Bouwmeester D 2003 *Phys. Rev. Lett.* **91** 130401
[20] Vitali D, Gigan S, Ferreira A, Böhn H R, Tombesi P, Guerreiro A, Vedral V, Zeilinger A and Aspelmeyer M 2007 *Phys. Rev. Lett.* **98** 030405
[21] Wang J, Tian X D, Liu Y M, Cui C L and Wu J H 2018 *Laser Phys.* **28** 065202
[22] Yan X B, Deng Z J, Tian X D and Wu J H 2019 *Opt. Express* **27** 24393
[23] Clark J B, Lecocq F, Simmonds R W, Aumentado J and Teufel J D 2017 *Nature* **541** 7636
[24] Asjad M, Abari N E, Zippilli S and Vitali D 2019 *Opt. Express* **27** 32427
[25] Marquardt F, Chen J P, Clerk A A and Girvin S M 2007 *Phys. Rev. Lett.* **99** 093902
[26] Guo Y J, Li K, Nie W J and Li Y 2014 *Phys. Rev. A* **90** 053841
[27] Liu Y M, Bai C H, Wang D Y, Wang T, Zheng M H, Wang H F, Zhu A D and Zhang S 2018 *Opt. Express* **26** 6143
[28] Li L C, Luo R H, Liu L J, Zhang S and Zhang J Q 2018 *Sci. Rep.* **8** 14276
[29] Lai D G, Zou F, Hou B P, Xiao Y F and Liao J Q 2018 *Phys. Rev. A* **98** 023860
[30] Zhang S, Zhang J Q, Zhang J, Wu C W, Wu W and Chen P X 2014 *Opt. Express* **22** 28118
[31] Liu Y L and Liu Y X 2017 *Phys. Rev. A* **96** 023812
[32] Gu K H, Yan D, Zhang M L, Yin J Z, Fu C B 2019 *Acta Phys. Sin.* **68** 054201 (in Chinese)
[33] Wu S C, Qin L G, Lu J, Wang Z Y 2020 *Chin. Phys. B* **28** 074204
[34] Cheng J, Liang X T, Zhang W Z and Duan X M 2018 *Chin. Phys. B* **27** 120302
[35] Zhang Y B, Liu J H, Yu Y F and Zhang Z M 2018 *Chin. Phys. B* **27** 074209
[36] Yan J K, Zhu X F and Chen B 2018 *Chin. Phys. B* **27** 074214
[37] Giovannetti V and Vitali D 2001 *Phys. Rev. A* **63** 023812
[38] Clerk A A, Devoret M H, Girvin S M, Marquardt F and Schoelkopf R J 2010 *Rev. Mod. Phys.* **82** 1155